INTERNAL REPORT #76

Geometry Factors and Other Data for the Heavy Isotope Spectrometer Telescope (HIST) on ISEE-3

by

R. A. Mewaldt

Space Radiation Laboratory
California Institute of Technology
Pasadena, California

10/3/80

I. Introduction

This internal report tabulates calculations of the geometry factors for the HIST experiment on ISEE-3. It also includes the physical dimensions of the telescope that served as the input data to the calculations, and summarizes inflight operation characteristics that affect HIST data analysis.

Two earlier documents (Garrard 1976, Althouse et al. 1978) contain earlier data of this type. In general these earlier reports were based on nominal dimensions and instrument performance characteristics. The present report supersedes these in using actual measured dimensions and in taking into account the inflight operation of the instrument. In particular:

a) Not all of the 24 x 24 matrix strips in M1 and M2 were operational at launch.

b) On December 1, 1978 there was a failure in the HIST readout logic. Subsequent to this the instrument was commanded into modes in which only a subset of the matrix strips are used, with a resulting reduction in geometry factor.

II. HIST History

HIST was in its normal operational mode from its initial turn-on (on 78:225) until the readout failure at ~ 78:335:2020. The following matrix strips were not operational at launch:

M1X1, M1Y1, M1Y24 in M1
M2X1, M2X24 in M2

Following the failure on 78:335, the instrument geometry remained the same until 79:053:1825, at which time the active M1 area was reduced to a 16 x 16 strip array, and M2 to an 8 x 8 array, each centered on the telescope axis. Later, at 79:079:2233 M2 was also changed to a 16 x 16 array. Table 3 summarizes these mode changes.

An additional failure that should be noted involves matrix strip M1Y16, which, according to quick-look data, stopped working between 79:055 and 79:059. It is not known to what extent this affects the response of M1, but a first approximation would suggest a ~ 12% reduction for the geometry factor during time period 2 and an ~ 6% reduction during time period 3. However, depending on the nature of this failure, some or even all M1Y16 events may trigger M1Y15 or M1Y17. This could be tested using flight data.

III. Physical Dimensions

Table 1 summarizes HIST detector dimensions. A schematic of the telescope is shown in Figure 1. The detector thicknesses for M1, M2, and D1 to D4 are based on analysis of flight proton data by H. Breneman. For other detectors the thicknesses correspond to nominal values and therefore may be in error by ≤ 5%. Detector active areas for M1 and M2 are based on an analysis of LBL Fe data by J. Spalding. For D1 through D3 and for D4 through D9 they are measured, or assumed, on the basis of average measurements of similar detectors. They are probably accurate to about 1%

Table 2 summarizes HIST detector spacings, as measured in the flight telescope by A. Cummings and K. Lau (report dated 5/17/78). Also given are the detector serial numbers (Ortec or Kevex), their SRL designations, and their orientation.

For operation modes of HIST subsequent to the instrument failure all physical data are the same except for the M1 and M2 active areas, as noted in Table 3.

IV. Geometry Factor Calculations

Geometry factors for Periods 1 and 2 were calculated using the IBM-370 program AOMA (by Stew Hartman), which uses the Monte-Carlo method. These results appear in Table 4. For these calculations M1 and M2 were approximated by circles of the area shown in Table 1. In order to eliminate edge effects it is often desirable to restrict the particle trajectories to a less than nominal D1 radius. Table 4 also includes geometry factors for a D1 radius of 1.31 cm.

For Periods 3 and 4 the geometry factors were calculated by the IBM-370 program SECHIST (originally developed by H. Breneman). SECHIST accepts arbitrary M1 and M2 sensitive dimensions (as individual mm^2 units) and then systematically considers all possible M1, M2 address combinations. SECHIST calculations for Periods 1 and 2 agree with AOMA results to within the statistical accuracy of the AOMA calculations.

An easy way to find the geometry factor at other locations (say the front of D5) is to plot geometry factor vs. distance below M1 and interpolate.

Table 5 includes the mean value of the secant of the zenith angle, and the rms standard deviation of the secant(theta) distribution.

V. Other HIST Documentation

SRL Internal Report #75 by H. Breneman considers the problem of identifying nuclei after the 12/1/78 readout failure. The geometry factors in Table 4 should be used in combination with his algorithms for computing absolute fluxes.

A brief and preliminary summary of the HIST readout failure is contained in a letter from E. C. Stone to T. von Rosenvinge on 4/18/79. This letter is attached as an appendix to this internal report.

VI. References

Althouse, W.E., A.C. Cummings, T.L. Garrard, R.A. Mewaldt, E.C. Stone, and R.E. Vogt, "A Cosmic Ray Isotope Spectrometer", IEEE Transactions on Geoscience Electronics, GE-16 (1978) 204.

Breneman, H., "Element and Isotope Identification from HIST Data Subsequent to the December 1, 1978 Readout Failure", SRL Internal Report #75 (1980).

Garrard, T.L., "Experiment Requirements Document for the Heavy-Isotope Spectrometer Telescope", SRL Technical Report 76-3 (1976).

Table 1 — HIST Detector Dimensions

Detector	SRL #	Serial number	Side* toward space	Thickness (microns)	Active Area (cm^2)	Active Radius (cm)
M1[†]	50-10	16-673A	Au	39	4.605	1.211
M2	50-11	16-673C	Au	41.5	4.710	1.224
D1	90-2	16-008D	Al	92	5.84[Δ]	1.363
D2	150-2	16-062D	Al	151	8.26[Δ]	1.621
D3	500-6	16-556B	Al	520	8.29[Δ]	1.624
D4	1.7-2	2214	UG	1570	9.08**	1.700
D5	3-10	2220	G	3000	9.12[Δ]	1.704
D6	3-4	2212	UG	"	9.24**	1.715
D7a	3-7	2217	G	"	9.12[Δ]	1.704
D7b	3-5	2213	UG	"	9.12[Δ]	1.704
D8a	3-1	2209	G	"	9.13**	1.705
D8b	3-9	2219	UG	"	9.12[Δ]	1.704
D9	3-8	2218	G	"	9.12[Δ]	1.704

---

* UG = ungrooved, G = grooved.

[†] The windows in front of M1 are equivalent to ∼ 15μm of silicon.

** Measured central area.

[Δ] Assumed central area, based on other similar detectors.

Table 2 — HIST Detector Spacings

Detector	Surface	Distance Below Top of M1 (cm)
M1	Al (front)	0.00
M2	Au (front)	4.973
D1	Al (front)	5.688
D2	Al (front)	6.097
D3	Al (front)	6.510
D4	UG (front)	6.846
	G (back)	7.030
D5	G (front)	7.132
	UG (back)	7.452
D6	UG (front)	7.621
	G (back)	7.943
D7 A	G (front)	8.043
D7 B	G (back)	8.700
D8 A	G (front)	8.804
D8 B	G (back)	9.456
D9	G (front)	9.556
	UG (back)	9.876

Table 3 — A History of HIST Operation Modes

Period #	Start	End	M1	M2	Comments
1	Launch	78:335:2019	24x24*	24x24*	Normal operation
2	78:335:2020	79:053:1824	24x24*	24x24*	Not all bits telemetered from here on
3	79:053;1825	79:079:2232	16x16†	8x8	Detectors D6, D7, D8 turned off
4	79:079:2233	present	16x16†	16x16	Detectors D6, D7, D8 turned off

---

* Note non-operational strips in Section II.

† M1Y16 failed sometime between 79:055 and 79:059.

Table 4 — HIST Geometry Factors

Range	Distance below M1 center (cm)	Period 1, 2 normal D1	Period 1, 2 "small" D1†	Period 3	Period 4
M1 center	0.0	8.7 (est)	8.7 (est)	5.0 (est)	5.0 (est)
M2 center	4.973	0.787 ± .008	0.787 ± .008	0.063 ± .001	0.248*
D1 center	5.691	0.728 ± .008	0.688 ± .007	"	0.248
D2 center	6.103	0.728 ± .008	0.688 ± .007	"	0.248
D3 center	6.534	0.715 ± .008	0.686 ± .007	"	0.248
D4 center	6.936	0.696 ± .008	0.673 ± .007	"	0.247
D5 center	7.290	0.657 ± .007	0.644 ± .007	"	0.245
D6 center	7.780	0.600 ± .007	0.592 ± .007	"	0.240
D7 center	8.370	0.528 ± .006	0.523 ± .006	——— Not Used ———	
D8 center	9.128	0.455 ± .006	0.452 ± .006		
D9 bottom	9.874	0.396 ± .006	0.393 ± .006		

---

† Small D1 radius = 1.31 cm, normal D1 = 1.364 cm.

* Absolute uncertainty ± 0.005, relative uncertainty ± 0.001.

Table 5 — Mean Values of Secant(theta)*

Range	Period 1, 2 normal D1	Period 1, 2 "small" D1	Period 3	Period 4
M2	1.0280 ± .0250	1.0280 ± .0250	1.0101 ± .0074	1.0161 ± .0135
D1	1.0247 ± .0225	1.0235 ± .0218	"	1.0161 ± .0135
D2	1.0247 ± .0225	1.0235 ± .0218	"	1.0161 ± .0135
D3	1.0238 ± .0215	1.0233 ± .0214	"	1.0161 ± .0135
D4	1.0226 ± .0203	1.0223 ± .0204	"	1.0160 ± .0134
D5	1.0206 ± .0189	1.0205 ± .0190	"	1.0157 ± .0129
D6	1.0181 ± .0172	1.0181 ± .0172	"	1.0150 ± .0121
D7	1.0155 ± .0152	1.0155 ± .0152		
D8	1.0129 ± .0136	1.0129 ± .0136		
D9	1.0110 ± .0123	1.0110 ± .0124		

---

* The uncertainty shown is the rms standard deviation of the secant(theta) distribution. It is not the uncertainty in the mean value.

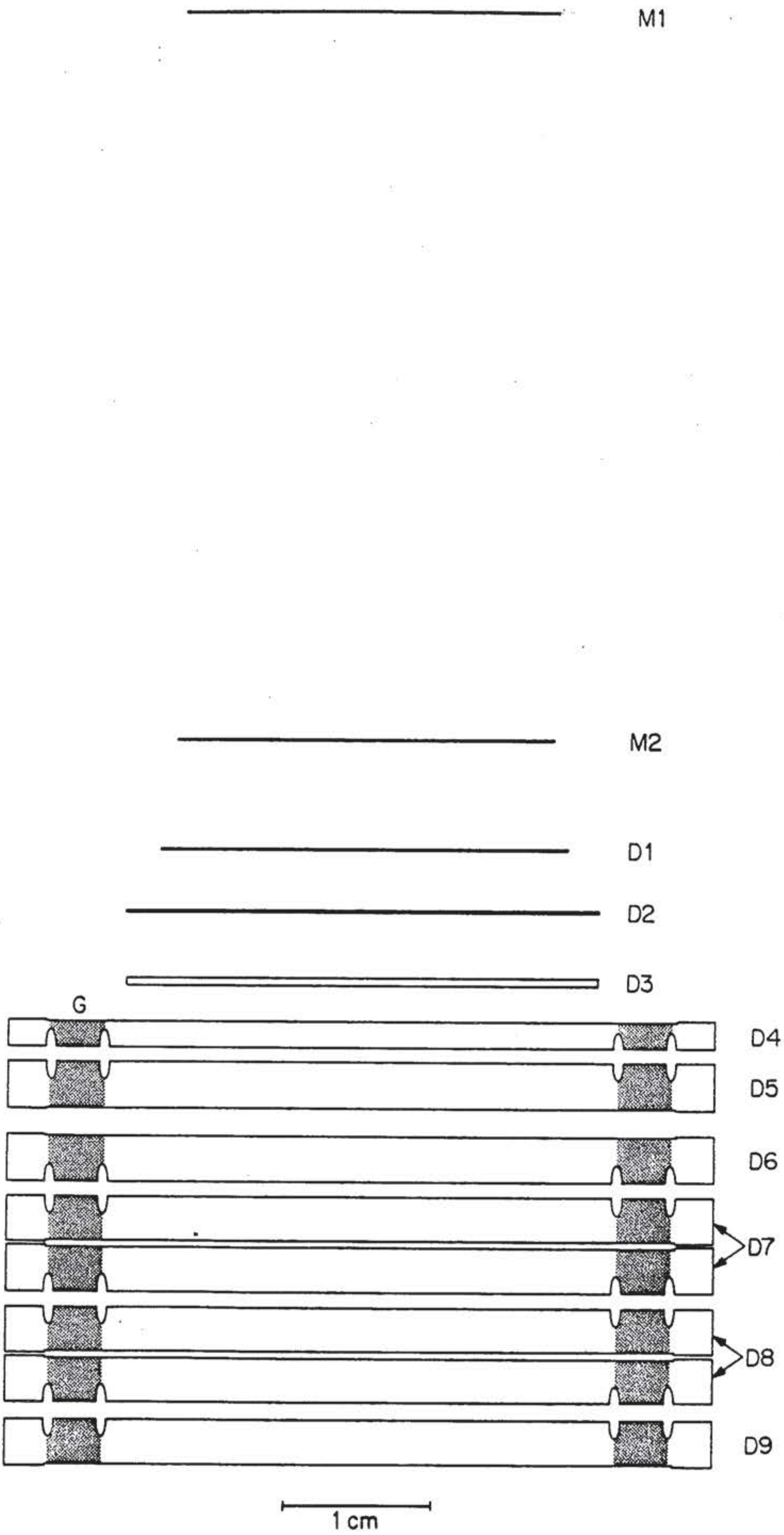

Figure 1

APPENDIX 1

CALIFORNIA INSTITUTE OF TECHNOLOGY
GEORGE W. DOWNS LABORATORY OF PHYSICS
PASADENA, CALIFORNIA 91125

18 April 1979

Dr. Tycho von Rosenvinge
ISEE-3 Project Scientist
Code 661
Goddard Space Flight Center
Greenbelt, Maryland 20771

Dear Tycho:

As you already are aware, there was a partial failure in the Caltech HIST readout logic in orbit. The attached report summarizes an engineering analysis of the failure, the resulting effect on HIST data readout, and a reconfigured command state for HIST. HIST has been operating in the revised command configuration since February 22, 1979. The following discussion assesses the impact of the failure and subsequent reconfiguration on future scientific results which may be expected from HIST.

Prior to this failure, HIST had full charge and isotope resolution for Z=1-28 events stopping in eight separate ranges. The necessary reconfiguration of the instrument disables the last three ranges (upper ~ 50% of the energy/nucleon coverage) and also reduces the geometry factor so that meaningful studies of galactic cosmic rays are probably limited to a supporting role (multi-spacecraft studies of long term spatial and temporal variations). On the other hand, the impact on event statistics for solar flare and interplanetary particles is actually minor, since these are by nature low energy particles, and since during large solar flares the event readout rate is independent of geometry factor.

We have just begun to analyze how to interpret the somewhat restricted pulse-height information now available from HIST. The following capabilities represent the minimum possible; further analysis should reveal more. The isotopes ^{1}H, ^{3}He and ^{4}He are individually identifiable over essentially the entire energy range. Even-Z elements from C(Z=6) through Si(Z=14) should be easily identifiable over most of the available energy interval. For heavier elements, including Fe, the available intervals where element identification is unambiguous constitute less than half of the total energy interval.

Although isotope analysis for Z>2 will be limited, it appears that over portions of each range the relative abundances of ^{20}Ne and ^{22}Ne, and ^{24}Mg, ^{26}Mg, and possibly ^{25}Mg can be determined. The equivalent mass resolution of the reconfigured HIST will be $\sigma_m \simeq 0.4$ amu at $Z \simeq 10$, with about one-half of the geometry factor having $\sigma_m \simeq 0.3$ amu. This mass resolution is sufficient for Ne and Mg where the less abundant species are $\geqslant 10\%$ of the main isotope and better than all other solar flare instruments. This should allow determination of an important question raised by earlier HIST data, namely, is the isotopic composition observed by HIST in the September 1978 flare also typical of flares with altered elemental composition. If so, these earlier measurements can be related to the composition of the solar atmosphere with more confidence.

Element identification and limited isotope resolution is still possible in HIST <u>only</u> because the location of the tracks of all isotopes is known precisely from pre-flight calibrations at the Bevalac and from in-flight flare observations. It is therefore possible to predict with confidence the possible bit combinations for each isotope as a function of energy, and then identify regions of unambiguous response. Note that the situation is helped considerably by the fact that HIST makes up to 5 separate energy loss measurements on each particle, thereby complimenting much of the information loss caused by missing bits.

In summary, although the capabilities of HIST to make high resolution isotope measurements have been severely compromised, the instrument can continue to do meaningful new science measuring solar and interplanetary elements and isotopes at 1 AU, and also serve as a baseline for the Voyager LET telescopes.

Sincerely,

Ed

E. C. Stone

ECS/v

PRELIMINARY REPORT ON THE LOGIC FAILURE IN HIST

On December 1, 1978, after 110 days in orbit, Caltech's Heavy Isotope Spectrometer Telescope (HIST) experiment aboard ISEE-3 experienced a component failure. This report will summarize the information developed to date on the nature and impact of the failure.

DESCRIPTION OF FAILURE

The failure has been traced to a single integrated circuit (I.C.), a CMOS CD4029 counter designated I11-09. This part contains the first four bits of an eight bit address counter which controls the address lines of the memories used to store HIST event data. The second counter stage of this part has become "monostable", resulting in a count sequence which proceeds 0,1,4,5, 8,9,12,13,16,17.... instead of 0,1,2,3,4...... The nature of the failure implies that the problem results from a defect on the chip itself; no external connections or bond wires are involved. No hypothesis for the defect has been suggested.

PART HISTORY

The part, a CD4029AK/1N, S/N D007398, was purchased by Caltech's manufacturing subcontractor, Time-Zero Laboratories (TZL) (now Ball Aerospace Systems Division, Western Laboratories) from DCA Reliability Laboratory of Mountain View, CA, on TZL's Purchase Order No. 11648, dated April 9, 1976. Forty seven pieces were ordered: 19 for the HIST instrument (TZL job number 2908) and 28 for another TZL contract (TZL job number 3903) with the University of California, Berkeley, for use on the UCB Heckman experiment also aboard ISEE-3. The parts were from a lot of 197 pieces purchased by DCA from RCA/Findley to RCA's/1N specification and then screened at DCA to an Ames Research Center screening specification, PS-201.

The lot of 197 parts purchased from RCA was shipped from three date codes - 106 pieces from d.c. 7605, 88 pieces from d.c. 7610, and 3 pieces from d.c. 7614; unfortunately, all subsequent processing of these parts failed to distinguish among these three date codes, so we don't know which of these three date codes was on the failed part. The parts were purchased from RCA with tinned leads.

Of the 19 pieces ordered for HIST, 15 are installed in the protoflight instrument, one was replaced after initial assembly due to poor solder wetting on leads, and 3 are left in residual stock, all date-coded 7605. Of the 28 pieces ordered for the UCB instrument, 18 are installed in the protoflight instrument and 10 pieces remain in residual stock, all from date code 7610. No electrical failures of CD4029's were experienced by either project prior to this incident in HIST.

After installation in HIST, S/N D007398 had more than 3615 hours of operation and had been through at least 23 temperature cycles with upper limits between +30°C and +65°C and lower limits between -10°C and -30°C. No anomalies were recorded prior to this failure.

IMPACT OF FAILURE

The failed part was one of 43 CMOS parts in the HIST logic design (out of approximately 500 CMOS parts total) which might be considered single-point failures in the sense that a failure could severely compromise the data returned from HIST. The direct result of this specific failure can be seen in Figure 1, HIST EVENT DATA FORMAT; the anomalous address sequence results in the loss of the data bits which have been bracketed (the remaining data bits are read out twice). Table I summarizes the impact on each data item of the original 128-bit data field. Read out of rate data is unaffected by this failure.

In order to limit ambiguities in the interpretation of the remaining event data bits, it is desirable to command the instrument into a reconfigured mode that concentrates on studies of solar flare and interplanetary heavy nuclei.

In essence, the reconfiguration does two things. First it disables the outer strips of each matrix detector plane, limiting the opening angle to $< 24^{0}$ for all data, but also permitting subsets of the data to be identified with more restricted variations in pathlength. Second, it prohibits analysis of events with Range 5 or greater so that the remaining Range identification bits may be unambiguously interpreted. Table II summarizes the instrument parameters for the reconfigured command state.

Figure 1 - HIST EVENT DATA FORMAT

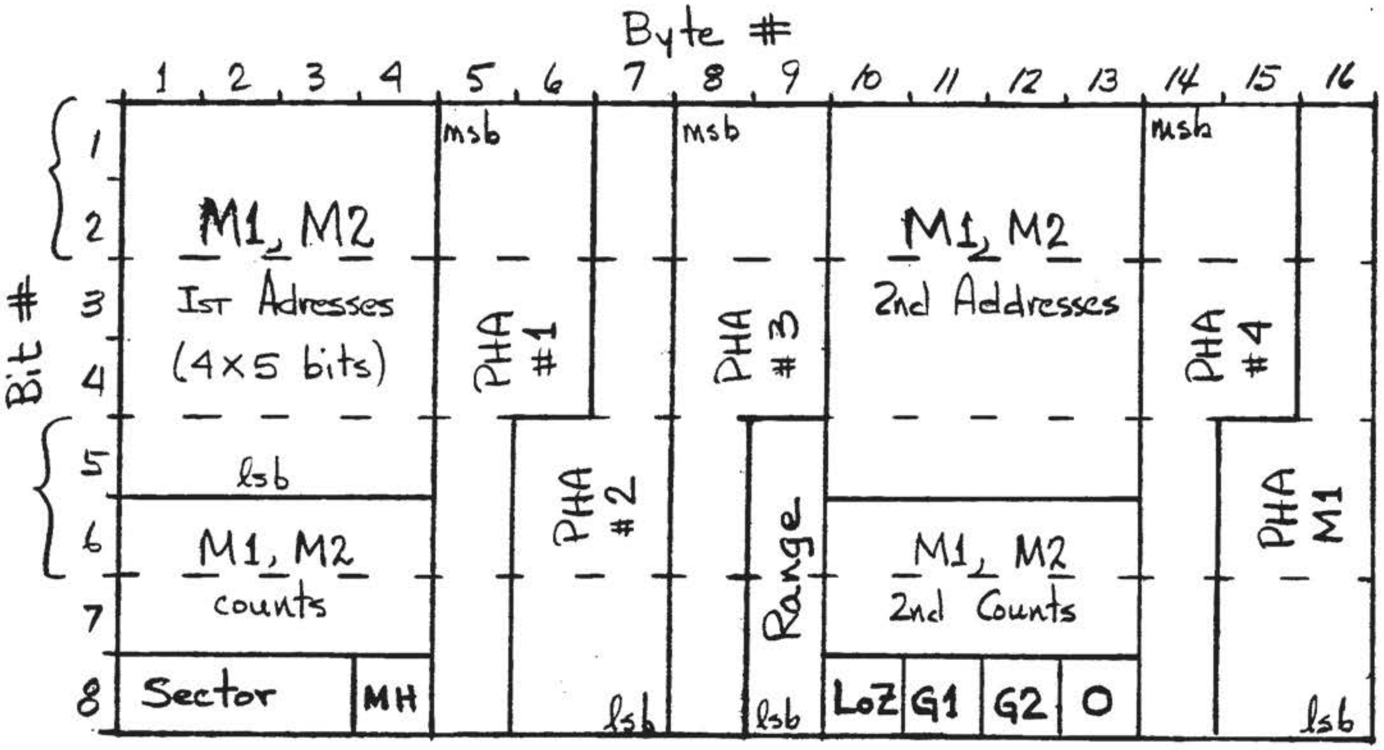

Note: Rows of bits (#1,2,5,6) within the brackets are presently lost.

TABLE I

Data Item	Present Status	Impact
Matrix 1st Addresses	lose 2/5 bits from each coordinate	Must disable some strips to reduce ambiguity
Matrix Counts	lose msb only	no appreciable impact
Sector	complete	none
MH (Multiple hodo)	ok	none - can still identify MH events
PHA's (5 of 12 bits each)	missing bits 3,4,7,8,11,12	PHA data is of lower resolution and "fragmented"
Range (stopping detector)	lose 2 msb's	Shut off D6,D7,D8 to remove ambiguity
Matrix 2nd Addresses and Counts	same as 1st addresses	None-these events not normally used.
LoZ (Z = 1,2)	ok	none
G1,G2 (guards)	ok	none

TABLE II

Parameters of the Reconfigured HIST Instrument

Parameter	Present Capability	Comments
Stopping event "Range"	M2 to D5	D6-D8 disabled
Energy Intervals	H = 2-11 MeV He = 2-32 MeV/nuc O = 5-70 " Fe = 6-130 "	~ ½ of original
Geometry Factor	0.25 $cm^2 \cdot sr$	~ 1/3 of original
Charge Identification		
Over ~ all of interval	Z = 1,2	
" ~ 2/3 " "	Z = 6-8,10,12,14	
" ~ 1/3 " "	Z = 16-26 (even Z)	
Isotope Identification		
Over ~ all of interval	Z = 1,2	
" ~ 1/3 " "	Z = 10,12	
Isotope Resolution	$\sigma_m \simeq 0.2$ amu (Z = 2) $\sigma_m \simeq 0.4$ amu (Z =10)	
Anisotropies	Six $Z \geq 3$ sectored rates Z = 1-28 events	
Position Information:	1) Pathlength, $\sigma_\ell/\ell < .015$ 2) Edge Effects ≐ none 3) Complete pileup and chance coincidence protection	(better in subsets of the data)
Multiparameter analysis	2 to 5 pulseheights for each event	
Rate data	Z = 1,2 $Z \geq 3$ seven energy intervals	
Problems to study:	Solar flare composition elemental Z = 1-26 isotopic Z = 2,10,12 Solar flare propagation + anisotropies Corotating Events - Composition, anisotropies Anomalous Component	